HSF1 as a Mitotic Regulator: Phosphorylation of HSF1 by Plk1 Is Essential for Mitotic Progression

Yoon-Jin Lee,[1] Eun-Ho Kim,[1] Jae Seon Lee,[2] Dooil Jeoung,[3] Sangwoo Bae,[1] Seung Hae Kwon,[4] and Yun-Sil Lee[1]

Divisions of [1]Radiation Effects and [2]Radiation Cancer Research, Korea Institute of Radiological and Medical Sciences, Seoul, Korea; [3]College of Natural Sciences, Kangwon National University, and [4]Korea Basic Science Institute, Chunchon Center, Chunchon, Korea

Abstract

Previously, heat shock factor 1 (HSF1) had been reported to induce genomic instability and aneuploidy by interaction with Cdc20. Here, we have further examined the functions of HSF1 in the regulation of mitosis. A null mutant or knockdown of HSF1 caused defective mitotic progression. By monitoring chromosomes in living cells, we determined that HSF1 was localized to the centrosome in mitosis and especially to the spindle poles in metaphase. HSF1 was phosphorylated by Plk1 at Ser^{216} of the DSGXXS motif during the timing of mitosis and a phospho-defective mutant form of HSF1 inhibited mitotic progression. Phosphorylated HSF1 during spindle pole localization underwent ubiquitin degradation through the $SCF^{\beta\text{-}TrCP}$ pathway. However, binding of HSF1 with Cdc20 stabilized the phosphorylation of HSF1. Moreover, $SCF^{\beta\text{-}TrCP}$–mediated degradation only occurred when phosphorylated HSF1 was released from Cdc20. HSF1 phosphorylation at Ser^{216} occurred in the early mitotic period with simultaneous binding of Cdc20. The interaction of HSF1 with $SCF^{\beta\text{-}TrCP}$ was followed and then the interaction of APC/Cdc20 was subsequently observed. From these findings, it was shown that Plk1 phosphorylates HSF1 in early mitosis and that the binding of phosphorylated HSF1 with Cdc20 and ubiquitin degradation by $SCF^{\beta\text{-}TrCP}$ regulates mitotic progression. [Cancer Res 2008;68(18):7550–60]

Introduction

Cell division is achieved by the progression through a series of events known as the cell cycle. To ensure that the original cell is copied with high fidelity, an elaborate control system using so-called checkpoints is used, preventing cell cycle events from occurring prematurely or in the wrong order. The checkpoint responsible for the appropriate metaphase to anaphase transition during mitosis is called the spindle assembly checkpoint. Its main role is to guarantee that each chromosome is properly attached to the spindle and that the spindle is functional before providing the signal to separate the sister chromatids. A failure to pass on the duplicated genetic material to both daughter cells contributes to cellular transformation, which in turn, might lead to cancer. To ensure proper segregation of chromosomes, mammalian cells undergo mitosis in a tightly controlled manner.

One of the major protein kinases involved in cell division and specifically in APC/C regulation is polo-like kinase 1 (Plk1). This kinase was first described in *Drosophila* (1) as a major mitotic regulator kinase. Plks are well-conserved in all of the eukaryotes and associate transiently with several mitotic structures including the spindle poles, kinetochores, the central spindle, and the midbody. Furthermore, Plk1 inactivation in mammalian cells has been found to induce a mitotic abnormality in generating aneuploidy (2). The maximal Plk1 kinase activity is reached in the G_2-M phase of the cell cycle, and the function of Plk1 is considered necessary for mitotic cellular events such as spindle formation, chromosome segregation, and cytokinesis (3).

Detailed studies have revealed that the involvement of Plk1 is crucial for the metaphase-anaphase transition. Most of these functions are linked to the regulation of the anaphase-promoting complex APC, an E3 ubiquitin ligase that is responsible for the timely destruction of various mitotic proteins, thereby regulating chromosome segregation, exit from mitosis, and a stable subsequent G_1 phase (4). The ancillary protein Cdc20, a targeting protein that contains a destruction box (D box) such as securine, first activates APC (5). Once APC-Cdc20 has initiated mitotic exit, Cdc20 itself is degraded and is replaced by Cdh1, allowing the degradation of a wider spectrum of substrates (6). One or more APC subunits (i.e., Apc1, Cdc27, Cdc16, and Cdc23) are phosphorylated during mitosis (7, 8) and dephosphorylation can inactivate mitotic APC (9). Therefore, the inhibition of Cdc20 defines an interval of cyclin stability and APC inactivity.

Heat shock transcription factor 1 (HSF1) has a key role in the cellular response leading to the expression of heat shock protein (*hsp*) genes under stress conditions (10). Upon stress, HSF1 undergoes trimerization, phosphorylation, and activation of DNA-binding activity, and activates *hsp* gene transcription through binding to heat shock elements present in the promoter regions of the *hsp* genes. However, recent studies suggest that the heat shock response becomes deregulated in cancer, and that HSF1 is expressed at a high level and has a role in carcinogenesis (11). A particularly distinctive feature of HSF1 resides in its dramatic redistribution during stress. Whereas the inactive factor displays a diffuse cytoplasmic and nuclear localization, it rapidly accumulates during stress in a few nuclear foci termed HSF1 granules. The role of HSF1 granules remains unclear (12–14). Although the presence of the granules correlates with the stress response, the granules do not form at sites of *hsp* gene transcription, and they are present in mitotic cells that have undergone heat shock that lack transcriptional activity, suggesting a role distinct from transcription regulation (14, 15). Quite unexpectedly, the number of HSF1 granules correlates with cell ploidy, thus supporting the existence of a specific chromosomal target (13, 14). There was a report describing that HSF1 granules form on chromosome 9 through a direct DNA-protein interaction with a specific subfamily of

Note: Supplementary data for this article are available at Cancer Research Online (http://cancerres.aacrjournals.org/).

Requests for reprints: Yun-Sil Lee, Division of Radiation Effects, Korea Institute of Radiological and Medical Sciences, 215-4 Gongneung-Dong, Nowon-Ku, Seoul 139-706, Korea. Phone: 82-2970-1325; Fax: 82-2970-2402; E-mail: yslee@kcch.re.kr.

©2008 American Association for Cancer Research.

doi:10.1158/0008-5472.CAN-08-0129

Downloaded from http://aacrjournals.org/cancerres/article-pdf/68/18/7550/2596139/7550.pdf by guest on 13 April 2024

satellite III repeats and that HSF1 granule formation requires both DNA-binding competence and the trimerization of the protein, and does not involve stress-induced chromosome modifications (16).

Previously, we have found that HSF1 directly binds to Cdc20 and affects APC activity, which results in aneuploidy production and genomic instability (17). In this study, we have further identified a novel function of HSF1 that is active in cancer cells under non–stress conditions, as a mitosis regulator with respect to its phosphorylation and degradation in regulation that influences mitotic behavior.

Materials and Methods

Plasmids and constructs. Wild-type human HSF1 was cloned into pHACE containing a COOH-terminal hemagglutinin tag (17). The phosphorylation mutant constructs HSF1 (S216A), HSF1 (S230A), HSF1 (S307A), HSF1 (S419A), HSF1 (S216N), and HSF1 (S216E) were constructed by using overlap extension primers. PCR products were digested with *Eco*RI and were cloned into the *Eco*RI sites of the pHACE vector. PCR products were also cloned into the pEGFP-N1 vector (BD Biosciences Clontech). The human β-TrCP1 full-length clone was purchased from RZPD. Plk1 and Plk1 dominant-negative mutants were kindly provided by Dr. J.S. Lee at the Korea Institute of Radiological and Medical Sciences (Seoul, Korea) and were then subcloned into the pCMV5-flag vector. A hemagglutinin-tagged ubiquitin plasmid was obtained from Dr. D.M. Kang (Korea Basic Science Institute, Chunchon Center, Chunchon, Korea).

Cell transfection. Predesigned small interference RNAs (siRNA) for human HSF1 (5′-GAACGACAGUGGCUCAGCAUU-3′), Plk1 (5′-CCUUGAUGAAGAAGAUCAC-3′), Mad2 (5′-TCCGTTCAGTGATCAGACA-3′), β-TrCP (5′-AGCUCUUGGUGGAUCAUCTT-3′), and a negative control (5′-UAGCGACUAAACACAUCAA-3′) were purchased from Dharmacon. Cells were transfected with the siRNAs by using Lipofectamine 2000 (Invitrogen) and with plasmids by the use of Lipofectamine Plus reagent and Lipofectamine reagent (Invitrogen) according to the manufacturer's guidelines.

Immunoblotting and immunoprecipitation. Immunoblotting and immunoprecipitation were performed essentially as previously described (18) using the following antibodies: anti-HSP27, -HSP70, -Cdc20, -Cdc27, -cyclin B1, -Cdc2, -GFP, -GST, -MAD2, β-TrCP (Santa Cruz Biotechnology), HSF1 (Neomarker), phosphohistone H3 (Abcam), hemagglutinin tag (Cell Signaling Technology), β-actin, and flag tag (Sigma). Four specific antibodies against the four phosphorylation sites of HSF1 (Ser^{216}, Ser^{230}, $Ser^{303/307}$, Ser^{419}) were generated using synthetic peptides produced by Peptron and were then affinity-purified.

Cell culture. HSF1 knockout mouse embryonic fibroblast (HSF1+/+ and HSF1−/− MEF) cells were kindly provided by Dr. Ivor J. Benjamin (University of Utah, Salt Lake City, UT). The cells were cultured in DMEM (Life Technologies), supplemented with heat-inactivated 10% fetal bovine serum (Life Technologies), 0.1 mmol/L of nonessential amino acids, glutamine, HEPES, and antibiotics at 37°C in a 5% CO_2 humidified incubator. The human non–small cell lung cancer cell lines NCI-H23, H358, H596, and H1299, and the human osteosarcoma cell line HOS were grown in RPMI 1640 supplemented with 10% fetal bovine serum, glutamine, HEPES, and antibiotics at 37°C in a 5% CO_2 humidified incubator.

Chemicals and reagents. MG132, thymidine, nocodazole, taxol, and cycloheximide were purchased from Calbiochem.

Flow cytometry. Cells were cultured, harvested, and fixed in 70% ethanol (1×10^6 cells/sample) for 30 min at 4°C. The cells were then washed twice with PBS and incubated in the dark for 10 min at 37°C in PBS containing 10 μg/mL of propidium iodide (Sigma) and 10 μg/mL of RNase A (Sigma). Flow cytometric analysis was performed using a FACScan flow cytometer (Becton Dickinson).

Kinase assays. Cell lysates were incubated with Plk1, BubR1 (PharMingen), Cdc2 (Santa Cruz Biotechnology) antibody, and immunocomplexes were collected on protein A-sepharose beads and resuspended in a kinase assay mixture containing [γ-^{32}P]ATP (NEN Life Sciences) and HSF1 protein (Stressgene) as substrates. Proteins were separated on SDS-polyacrylamide gels, and the protein bands were detected by autoradiography.

Immunofluorescence analysis. Cells were grown on chamber slides (LabTakII; Nunc). After transfection or drug treatment, cells were washed twice with PBS, fixed in 4% paraformaldehyde, washed with PBS, and were then incubated for 30 min with 0.01% Triton X-100 in PBS. The cells were then incubated with 1 μg/mL of anti-HSF1. The cells were also stained with a 1:2,000 dilution of human CREST autoimmune serum (ImmunoVision) or antitubulin (Santa Cruz Biotechnology) antibody. After washing, fluorescent secondary antibodies (Molecular Probes, Invitrogen) were added at a 1:500 dilution. The cells were again washed with PBS, counterstained with 4,6-diamidino-2-phenylindole dihydrochloride (DAPI), and were imaged under a confocal laser-scanning microscope (Leica Microsystems).

Time-lapse microscopy. For live-cell imaging, H2B-GFP–transfected cells were placed in microincubation chambers (Olympus IX-IBC) on the stage of an Olympus IX-71 microscope, which was heated to 37°C and equipped with a CO_2 supply and a charge-coupled device camera (Olympus Cool SNAP cf color 10L). The cooled charge-coupled device camera was controlled using PVCAM 2.6.3 software (Olympus). Time-lapse photographs were obtained using 5-min intervals, converted to 8-bit images, and processed using Adobe Photoshop 5.5 software.

Binding assays *in vitro*. The *in vitro* transcription and translation reactions of β-TrCP were performed using a TNT T7 Quick Master Mix kit (Promega) in the presence of [^{35}S]methionine, according to the manufacturer's protocol. Hemagglutinin-HSF1 immunocomplexes were then incubated with 5 μL of β-TrCP and *in vitro* translated in 500 μL of NETN buffer [100 mmol/L NaCl, 1 mmol/L EDTA (pH 8.0), 20 mmol/L Tris-HCl (pH 8.0), 0.2% NP40, and 10 mmol/L imidazole] for 2 h. Beads were washed five times with 1 mL of NETN buffer, resuspended in Laemmli sample buffer, and subjected to SDS-PAGE prior to autoradiography.

***In vitro* ubiquitinylation assay.** *In vitro* assays of the ubiquitination products of HSF1 were performed as previously described (19). In brief, Plk1-transfected cell lysates were incubated for 1 h at 4°C with *in vitro*–translated HSF1 (5 μL) that had been preincubated for 30 min at 4°C. After being washed twice, immunoprecipitates were then supplied with purified UbcH10 (Calbiochem), E1 (Calbiochem), an ATP-regenerating system [7.5 mmol/L creatine phosphate, 1 mmol/L ATP, 1 mmol/L $MgCl_2$, 0.1 mmol/L EGTA, and rabbit creatine phosphokinase type I (30 units mL^{-1}; Sigma)], ubiquitin (1.25 mg/mL; Sigma), and a ^{35}S-labeled *in vitro*–translated fragment of cyclin B. The reactions were stopped after 60 min at 25°C, and the extent of substrate ubiquitinylation was determined by SDS-PAGE and autoradiography.

***In vivo* ubiquitinylation assays.** Cells transfected with a plasmid-encoding hemagglutinin-tagged human ubiquitin were subjected to thymidine block and release and were then analyzed for ubiquitinylation *in vivo* as previously described (19). The cells were lysed by incubation for 10 min at 37°C with 2 volumes of TBS [10 mmol/L Tris-HCl (pH 7.5), and 150 mmol/L NaCl] containing 2% SDS. After adding 8 volumes of 1% Triton X-100 in TBS, lysates were sonicated for 2 min, and were incubated with protein G-agarose beads, which were then removed by centrifugation. The lysates were then immunoprecipitated with anti-HSF1 coupled to protein G-agarose. The beads were washed twice with 0.5 mol/L of LiCl in TBS, washed twice with TBS, boiled, and immunoblotted using antihemagglutinin.

Results

HSF1 is required for orderly mitotic progression. To investigate the function of endogenous HSF1 in mitotic progression, we used HSF1+/+ and HSF1−/− murine fibroblast cells (MEF). MEF cells stably expressing GFP-tagged histone H2B were used for live-cell imaging as shown in Fig. 1*A*. The image shows the indicated time points after the start of chromosome condensation at 12 hours of thymidine block and release. HSF1−/− MEF cells showed massive chromosome missegregation without the organization of the chromosomes in a metaphase plate, whereas HSF1+/+ cells exhibited completed division of

Downloaded from http://aacrjournals.org/cancerres/article-pdf/68/18/7550/2596139/7550.pdf by guest on 13 April 2024

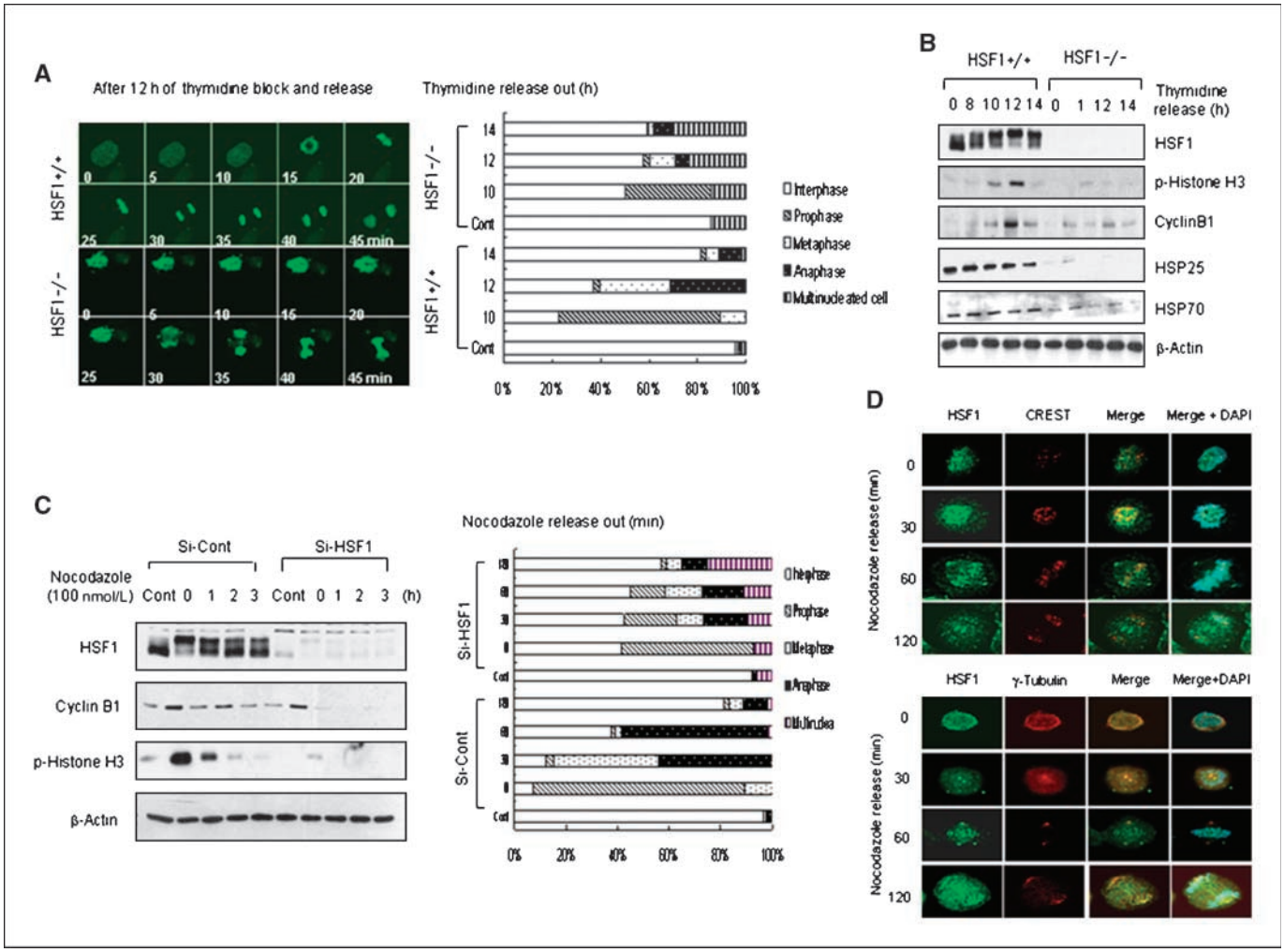

Figure 1. HSF1 is required for orderly mitotic progression. *A,* H2B-GFP–transfected HSF1+/+ and HSF1−/− MEF cells were synchronized by a double thymidine block and were released from the block into fresh medium. Mitotic progression was detected by time-lapse microscopy (*left*). HSF1+/+ and HSF1−/− MEF cells were synchronized by a double thymidine block and were released from the block into fresh medium. The DNA morphology was then analyzed by DAPI staining, and cells were classified. The histograms summarize the results of three independent experiments (with at least 400 cells counted in each experiment in each column; *right*). *B,* HSF1+/+ and HSF1−/− MEF cells were harvested at the indicated times following release from the double thymidine block, and lysates were generated for immunoblot analysis. *C,* control or HSF1 siRNA-transfected HOS cells were harvested at the indicated times following release from a nocodazole block (100 nmol/L nocodazole, 16 h). Cell lysates were analyzed using the indicated antibodies (*left*). The percentage of cells in each mitotic phase was determined by DAPI staining. A minimum of 400 transfected cells were counted per sample in three independent experiments (*right*). *D,* HOS cells were released from nocodazole (100 nmol/L) arrest after 16 h and stained for CREST (*red*), HSF1 (*green*), and DAPI. Cells were analyzed using immunofluorescence microscopy at different mitotic stages.

chromosomes from metaphase to anaphase (Fig. 1*A, left*). When the percentages of cells in prophase, metaphase, and anaphase were measured, HSF1−/− cells did not show any proper mitotic progression, which resulted in a high percentage of multinucleated cells; however, HSF1+/+ cells did progress normally (Fig. 1*A, right*). In addition, HSF1−/− MEF cells showed reduced phosphorylation of histone H3, a mitosis marker which indicates that HSF1 is essential to undergo mitotic entry after thymidine double block and release. When compared with HSF1+/+ cells, HSF1−/− MEF cells showed a decreased level of cyclin B1 and securine (data not shown; Fig. 1*B*), suggesting that HSF1 is also required for proper mitotic progression. HSF1+/+ cells showed high expression of the HSPs such as inducible HSP70 and HSP25, when compared with expression in HSF1−/− cells, as indicated previously (20). However, our previous findings have suggested that HSF1 in mitotic regulation was not dependent on the expression of HSPs (17). When we treated HOS cells which show high expression of HSF1 with a control RNA (Si-Cont) or HSF1-siRNA (Si-HSF1) and then create a nocodazole block and release, Si-HSF1 reduced the phosphorylation of histone H3 (at Ser^{10}), as well as the phosphorylation of HSF1, when compared with the effect in Si-Cont–treated cells (Fig. 1*C, left*). Moreover, treatment with Si-HSF1 inhibited proper mitotic progression with a high percentage of multinucleated cells (Fig. 1*C, right*), suggesting that HSF1 is essential for the mitotic process. Treatment with taxol or nocodazole, which are commonly used to probe spindle assembly checkpoint function by blocking microtubule attachment or by causing a microtubule dynamics–induced mitotic arrest in HSF1+/+ cells, did not have such effects in HSF1−/− cells. Defective mitotic arrest after treatment of these drugs in HSF1−/− cells resulted in a significantly increased number of multinucleated cells (Supplementary Fig. S1). These results strongly suggest that

Downloaded from http://aacrjournals.org/cancerres/article-pdf/68/18/7550/2596139/7550.pdf by guest on 13 April 2024

HSF1 is also required for spindle assembly checkpoint function. To further elucidate the function of HSF1 in mitotic cell cycle regulation, HOS cells were treated with nocodazole block and release. The appearance and degradation of phosphorylation of HSF1 was shown in a mitosis-dependent manner (data not shown). We examined the subcellular localization of endogenous HSF1 in HOS cells using immunofluorescence microscopy. Anti-HSF1 produced staining of the kinetochore region on the mitotic chromosomes. Kinetochore staining was confirmed by colocalization with CREST. From prometaphase through anaphase, HSF1 showed prominent centrosome localization, as judged by costaining for γ-tubulin. Moreover, the distribution of HSF1 was clearly concentrated to the spindle pole in metaphase (Fig. 1*D*). These results indicate that phosphorylation and distribution of HSF1 occurs in a mitotic phase–dependent manner.

Plk1 phosphorylates Ser^{216} of HSF1 in mitosis. To elucidate the mechanism that regulates phosphorylation of HSF1 in mitosis, we first examined several protein kinases such as Plk1, BubR1, Cdc2, and Aurora A kinase (ARK), which are the major protein kinases that regulate mitosis. Immunoprecipitation analysis showed that Plk1 from nocodazole-arrested mitotic cells directly phosphorylated HSF1 *in vitro*, but other mitotic kinases such as BubR1, Cdc2, and ARK did not (Fig. 2*A*). The interaction between Plk1 and HSF1 in mitotic cells was observed at a higher level when

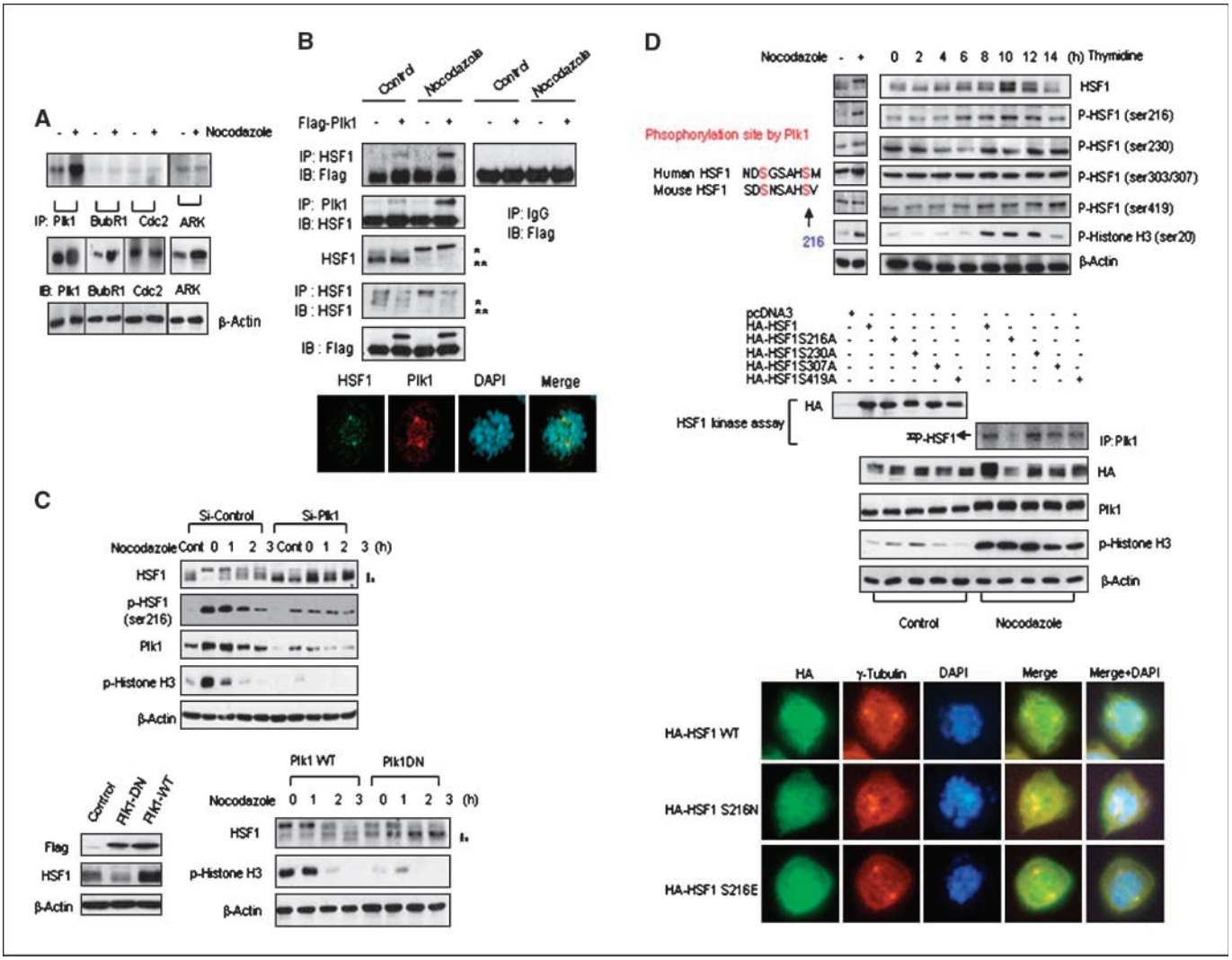

Figure 2. Phosphorylation of HSF1 at Ser^{216} by Plk1 in mitosis. *A,* cells were synchronized in mitosis by treatment with nocodazole (100 nmol/L nocodazole, 16 h). The mitotic cells were harvested and lysates were generated for a kinase assay and immunoblotting. *B,* cells transiently transfected with control or flag-tagged wild-type Plk1 were synchronized in mitosis by treatment with nocodazole (100 nmol/L nocodazole, 16 h). The mitotic cells were harvested and lysates were generated for immunoprecipitation and immunoblotting (*top*). Cells were processed for immunoflourescence using anti-HSF1 and anti-Plk1 antibodies, and were labeled with DAPI to stain DNA (*bottom*). *C,* cells were transiently transfected with control or Plk1 siRNA (*top*) or with flag-tagged wild-type Plk1 or a dominant-negative Plk1 (*bottom*), harvested at the indicated times following release from a nocodazole block (100 nmol/L nocodazole, 16 h), and lysates were generated for immunoblotting. *D,* conserved HSF1 amino acid regions corresponding to the Plk1 phosphorylation site (DSGXXS motif; *top left*). HOS cells were treated with nocodazole for 16 h. Cells were harvested at the indicated times following double thymidine block and were released from the block. Cell lysates were subjected to immunoblotting using phospho-HSF1 antibodies (*top right*). Mitotic cells treated with nocodazole were immunoprecipitated with anti-Plk1. Anti-Plk1 immunoprecipitates were subjected to a kinase assay. *In vitro*–translated proteins from hemagglutinin-tagged HSF1 (S216A, S230A, S307A, and S419A) plasmids were used as substrates. Hemagglutinin-tagged HSF1 (S216A, S230A, S307A, and S419A) transfected cells were treated with nocodazole for 16 h and lysates were subjected to immunoblotting (*middle*). HOS cells were transfected with hemagglutinin-tagged wild-type HSF1, S216N, or S216E. Cells were immunostained for detection of hemagglutinin (*green*) and γ-tubulin (*red*). DNA was stained with DAPI. Colocalization of proteins was analyzed by confocal microscopy (*bottom*).

Downloaded from http://aacrjournals.org/cancerres/article-pdf/68/18/7550/2596139/7550.pdf by guest on 13 April 2024

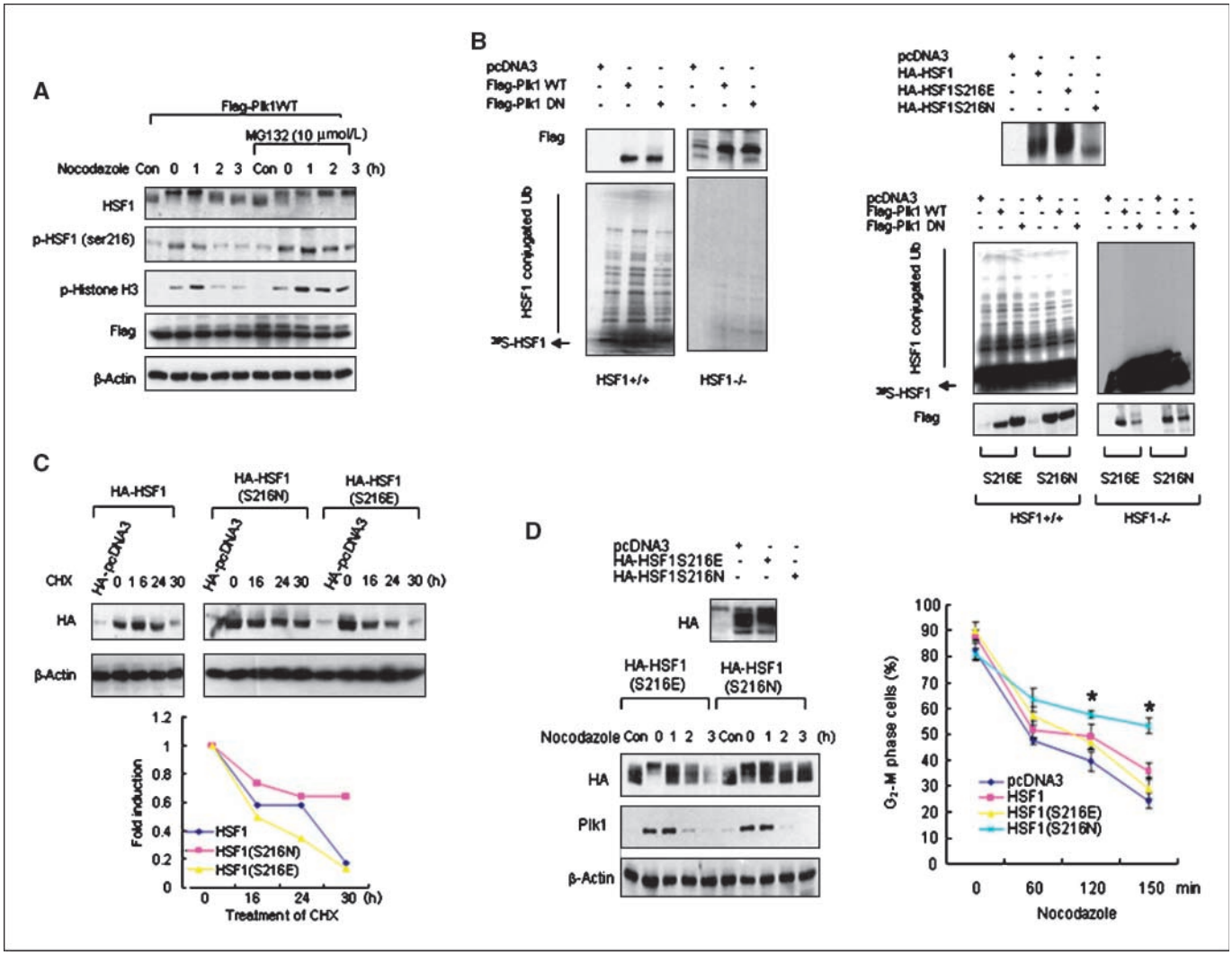

Figure 3. Phosphorylation of HSF1 at Ser^{216}-dependent ubiquitinylation and degradation. *A,* nocodazole-arrested cells were released into fresh medium or medium containing a proteasome inhibitor (*MG132*). Cells were harvested at the indicated times following release from a nocodazole block (100 nmol/L nocodazole, 16 h) and lysates were subjected to immunoblotting. *B,* HSF1+/+ and HSF1−/− MEF cells were transfected with vectors for Flag wild-type or dominant-negative Plk1 and were harvested after 18 h from a thymidine block (2 mmol/L thymidine, 16 h). Cell lysates were immunoprecipitated with anti-Flag. The resulting precipitates were analyzed using anti-ubiquitin. HOS cells were transfected with vectors for Flag wild-type or dominant-negative Plk1 and were harvested after a nocodazole block (100 nmol/L nocodazole, 16 h). Wild-type and dominant-negative Plk1 were purified from mitotic cells with anti-Flag and were assayed for ubiquitin ligase activity using a [^{35}S]-labeled *in vitro*–translated HSF1. The relative amounts of Plk1 protein in the reaction mixtures were also determined by immunoblotting with anti-Flag (*left*). HSF1+/+ and HSF1−/− MEF cells were transfected with vectors for Flag wild-type or dominant-negative Plk1 and were harvested after a nocodazole block (100 nmol/L nocodazole, 16 h). Wild-type and Plk1 were purified from mitotic cells with anti-Flag and assayed for ubiquitin ligase activity using a [^{35}S]-labeled *in vitro*–translated HSF1 (wild-type, S216E, and S216N). [^{35}S]-labeled *in vitro*–translated HSF1 proteins were also identified by autoradiography (*right*). *C,* HOS cells were transiently transfected with hemagglutinin-HSF1 (wild-type, S216E, and S216N) and cycloheximide (10 μg/mL) was added to block protein synthesis. Cells were harvested at the indicated times and lysates were analyzed by immunoblotting with antihemagglutinin for HSF1 levels (*top*) and quantified by densitometry (*bottom*). *D,* HOS cells were transiently transfected with hemagglutinin-HSF1 (S216E and S216N). Cells were harvested at the indicated times following release from a nocodazole block (100 nmol/L nocodazole, 16 h; *left*) and lysates were subjected to immunoblotting. Cellular DNA content was determined by flow cytometry (*right*).

compared with the control cells (Fig. 2*B, top*). Moreover, Plk1 was also colocalized with HSF1 to the spindle poles during prometaphase (Fig. 2*B, bottom*). When we examined these phenomena in Plk1-siRNA–treated HOS cells, proper mitotic progression was inhibited (no spindle poles were observed) and no HSF1 localization was observed (data not shown). Plk1-siRNA treatment inhibited HSF1 phosphorylation and transfection of a Plk1 dominant-negative mutant (Plk1DN) also showed similar results that coincided with the inhibition of phospho-histone H3 after nocodazole treatment (Fig. 2*C*), indicating that HSF1 was phosphorylated by Plk1 in the mitotic period. When Plk1 localization during mitotic cell cycle progression of HSF1−/− MEF cells was examined, improper localization of Plk1 and the presence of multinucleated cells were observed (Supplementary Fig. S2). It is well known that HSF1 is phosphorylated at several serine residues and Ser^{216} of HSF1 lies in a consensus region for the Plk1 phosphorylation site (E/D-X-S/T). We therefore tested whether Plk1 directly phosphorylates Ser^{216} of HSF1. Endogenous phosphorylation of HSF1 in HOS cells was determined with antibodies directed against phosphopeptides. Ser^{216} was markedly phosphorylated in nocodazole-induced mitotic cells, whereas Ser^{230} and Ser^{419} were not phosphorylated. Phosphorylation of Ser$^{303/307}$

Downloaded from http://aacrjournals.org/cancerres/article-pdf/68/18/7550/2596139/7550.pdf by guest on 13 April 2024

occurred independently of the phase of the cell cycle. Phosphorylation of HSF1 at Ser^{216} occurred temporally during mitosis that was detected using a phospho-histone H3 antibody and disappeared soon after the mitotic period when a thymidine double block and release was performed. In the case of other phosphorylation residues for HSF1 such as Ser^{230}, $Ser^{303/307}$, and Ser^{419}, no critical changes were found during mitosis (Fig. 2*D, top*). Treatment of antibodies with each peptide abolished specific protein bands on a Western blot, indicating that antibodies against phosphopeptides recognized specific phosphorylation sites of HSF1 (data not shown). When a Plk1 kinase assay was performed using HSF1 as a substrate, Plk1 did not phosphorylate the HSF1S216A mutant in mitosis but other mutants such as HSF1S230A, HSF1S307A, and HSF1S419A were phosphorylated. In addition, HSF1 phosphorylation was not observed in mitotic cells when the HSF1S216A mutant was transfected, whereas in the case of the other mutants, HSF1 phosphorylation in mitosis was easily observed (Fig. 2*D, middle*). From these findings, we strongly suggest that Plk1 directly phosphorylates the Ser^{216} residue of HSF1 in the mitotic period. To define the phosphorylation-dependent distribution of HSF1, hemagglutinin-tagged HSF1WT, HSF1S216N, or HSF1S216E mutants were transfected into HOS cells. Compared with HSF1WT and the HSF1S216E mutant (phospho-mimic form), the HSF1S216N mutant (phospho-defective mutant form) remarkably diminished the spindle pole localization (Fig. 2*D, bottom*), indicating that phosphorylation of HSF1 by Plk1 is critical for the localization of HSF1 to the spindle pole. However, overexpression of HSF1 resulted in diffuse localization on the kinetochore. These results support the hypothesis that phosphorylation-dependent spindle pole localization of HSF1 by Plk1 leads the completed cell division through proper chromosome alignment at metaphase.

Phosphorylated HSF1 at Ser^{216} induces ubiquitin degradation. Because phosphorylated HSF1 seemed to be degraded faster as compared with the unphosphorylated form during mitosis progression, the protein stability of phosphorylated HSF1 was examined. When we synchronized the cells by the use of a nocodazole block and release after transfection of Plk1WT, treatment with a proteasome inhibitor (MG132) during nocodazole release sustained the phosphorylation status of HSF1 and inhibited the degradation of HSF1, when compared with the effect on MG132

Downloaded from http://aacrjournals.org/cancerres/article-pdf/68/18/7550/2596139/7550.pdf by guest on 13 April 2024

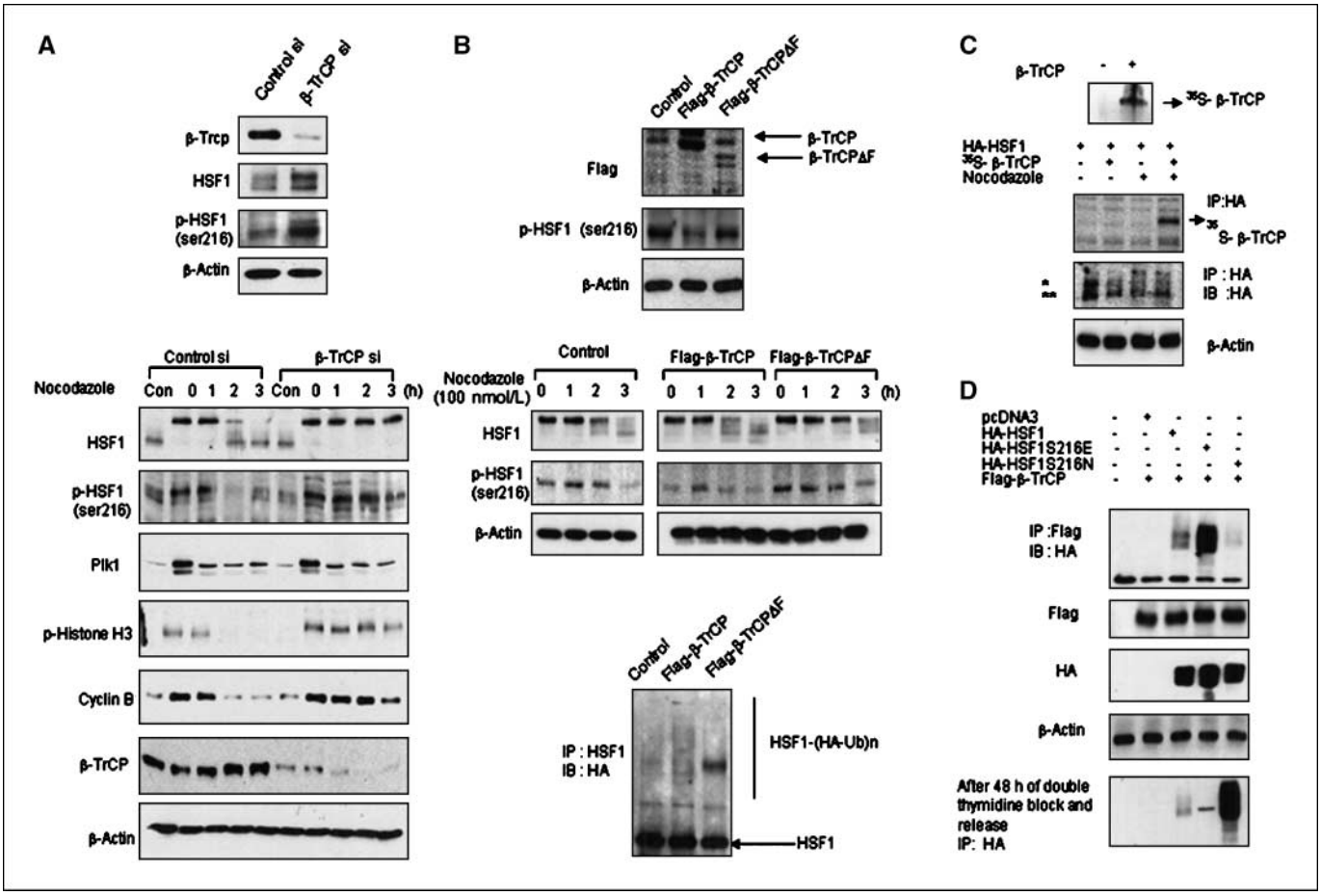

Figure 4. The β-TrCP–dependent pathway for phosphorylated HSF1 destruction. *A,* HOS cells were treated with control or β-TrCP siRNA. Cells were harvested at the indicated times following release from a nocodazole block (100 nmol/L nocodazole, 16 h) and lysates were subjected to immunoblotting. *B,* HOS cells were treated with Flag-tagged β-TrCP or β-TrCPΔF (*top*). Cells were harvested at the indicated times following release from a nocodazole-block (100 nmol/L nocodazole, 16 h) and the lysates were subjected to immunoblotting (*middle*). HOS cells were cotransfected with vectors for hemagglutinin-ubiquitin and β-TrCP or β-TrCPΔF. Cell lysates were immunoprecipitated with anti-HSF1. The resulting precipitates were analyzed using antihemagglutinin (*bottom*). *C,* HOS cells were transfected with hemagglutinin-HSF1 and treated with nocodazole (100 nmol/L nocodazole, 16 h). *In vitro*–translated [^{35}S]-labeled β-TrCP was incubated with hemagglutinin-HSF1 immunoprecipitates and subjected to an *in vitro* binding assay. *D,* HOS cells were cotransfected with Flag-β-TrCP and hemagglutinin-HSF1 (wild-type, S216E, and S216N). Cell lysates were subjected to immunoprecipitation and immunoblotting. Degradation of HSF1 (wild-type, S216E, and S216N) was detected by the use of antihemagglutinin after 48 h of double thymidine block and release.

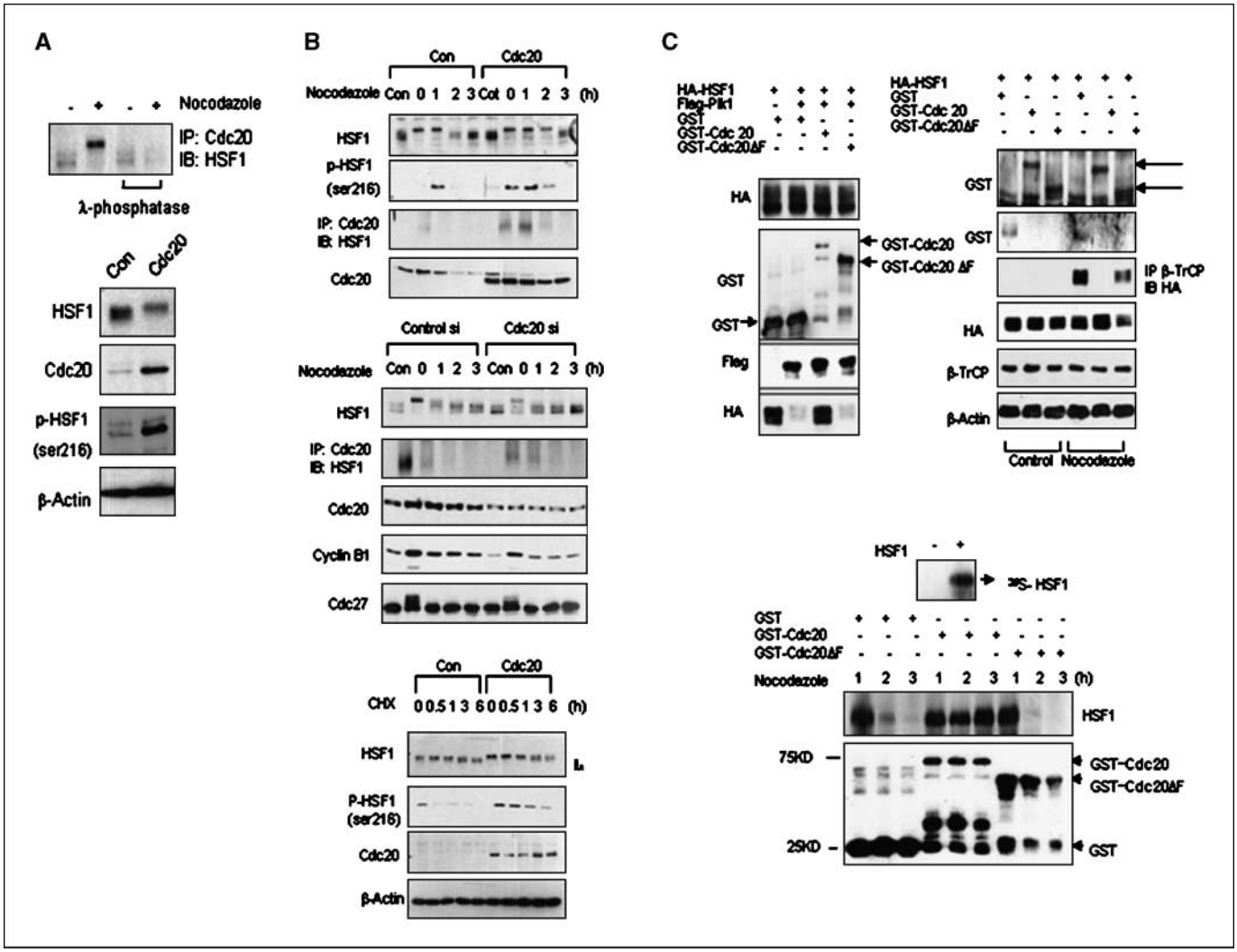

Figure 5. Cdc20 controls phosphorylated HSF1 stability by blocking recruitment of β-TrCP to phosphorylated HSF1. *A,* Cdc20 immunoprecipitated from M phase HOS cell lysates was incubated with or without λ-phosphatase and immunoblotted with anti-HSF1 (*top*). Cdc20 overexpressed cell lysates were immunoblotted with the indicated antibodies (*bottom*). *B,* Cdc20-overexpressed cells were harvested at the indicated times following release from a nocodazole block (100 nmol/L nocodazole, 16 h) and lysates were subjected to immunoprecipitation and immunoblotting (*top*). Control or Cdc20 siRNA–treated cells were harvested at the indicated times following release from a nocodazole block (100 nmol/L nocodazole, 16 h) and lysates were subjected to immunoprecipitation and immunoblotting (*middle*). Cdc20-overexpressed cells were harvested at the indicated times from cycloheximide (10 μg/mL) treatment and lysates were subjected to immunoprecipitation and immunoblotting (*bottom*). *C,* hemagglutinin-HSF1–overexpressed cells were cotransfected with a GST control, Cdc20 or Cdc20ΔF, and Flag-Plk1. Degradation of HSF1 was detected by the use of antihemagglutinin after 48 h of double thymidine block and release (*top left*). HOS cells were harvested at the indicated times following release from a nocodazole block. GST, GST-Cdc20, or GST-Cdc20ΔF proteins were incubated with ^{35}S-labeled HSF1 in mitotic HOS cell lysates for 2 h at 37°C. The reaction mixture was analyzed by SDS-PAGE and autoradiography (*top right*). HOS cells were cotransfected with hemagglutinin-HSF1 and GST control, GST-Cdc20, or GST-Cdc20ΔF and were then treated with nocodazole (100 nmol/L nocodazole, 16 h). The cell lysates were subjected to immunoprecipitation and immunoblotting (*bottom*).

untreated control cells. Prolonged phosphorylation of HSF1 at Ser^{216} was also observed, as well as prolonged expression of phospho-histone H3. Therefore, phosphorylation of HSF1 at Ser^{216} is accompanied by protein degradation (Fig. 3*A*). *In vivo* HSF1 ubiquitination was examined in cells expressing hemagglutinin-HSF1 and Plk1WT or Plk1DN. Figure 3*B* shows that ubiquitinylation of HSF1 requires the protein kinase activity of Plk1 in HSF1+/+ MEF cells, given that no significant ubiquitinylation was observed with a kinase-defective Plk1 mutant (Plk1DN); however, ubiquitinylation was observed with wild-type Plk1 (Plk1WT). In the case of HSF1−/− cells, no ubiquitinylation of HSF1 was observed (Fig. 3*B, left*). We then reconstituted a Plk1-mediated ubiquitination assay *in vitro* and directly tested the ability of HSF1 ubiquitinylation to serve as a substrate for Plk1. Plk1-stimulated ubiquitinylation of HSF1 was also prevented by a mutation at S216N and slightly augmented by a mutation at S216E of HSF1 in HSF1+/+ MEF cells (Fig. 3*B, right*). From these results, we concluded that the ligation of HSF1 to ubiquitin requires phosphorylation of HSF1 at Ser^{216} by Plk1. To directly measure the effect of phosphorylation at Ser^{216} on HSF1 protein stability, HOS cells transfected with HSF1WT, the S216N HSF1 mutant and the S216E HSF1 mutant were arrested in S phase by use of a double thymidine block. The cells were then released into fresh medium containing cycloheximide to inhibit new protein synthesis. As compared with the wild-type and the S216E HSF1 mutant, the stability of the S216N HSF1 mutant was increased (Fig. 3*C*). We also examined whether other

Downloaded from http://aacrjournals.org/cancerres/article-pdf/68/18/7550/2596139/7550.pdf by guest on 13 April 2024

phosphorylation sites of HSF1 affect the protein stability of HSF1. The S230A HSF1 mutant degraded faster than the S216A HSF1 mutant (Supplementary Fig. S3). In addition, as compared with the S216E HSF1 mutant, degradation of S216N was inhibited after nocodazole block and release (Fig. 3*D, left*). Cell cycle studies also suggested that stabilization of HSF1 by the S216N HSF1 mutant coincided with mitotic arrest after nocodazole block and release (Fig. 3*D, right*), indicating that proper destruction of the phospho-HSF1 at Ser^{216} is necessary for mitotic exit. When the phosphorylation status of HSF1 in mitosis was sustained by treating cells with okadaic acid, a phosphatase inhibitor, an increased G_2-M phase arrest was observed (Supplementary Fig. S4).

Destruction of phosphorylated HSF1 by the $SCF^{\beta\text{-TrCP}}$–dependent pathway. Recent reports have shown that the serine residues in the DSGXX(X)S region (in which X represents any amino acid) must be phosphorylated to allow recognition by $SCF^{\beta\text{-TrCP}}$ (β-TrCP; ref. 21). To examine whether degradation of phosphorylated HSF1 occurs by the action of β-TrCP, we used siRNA to reduce the expression of β-TrCP in HOS cells. Depletion of β-TrCP inhibited the degradation of phosphorylated HSF1 after nocodazole block and release. Phosphorylation of HSF1 at Ser^{216} was also sustained after β-TrCP-siRNA transfection, as well as the prolonged expression of phospho-histone H1 and cyclin B1 (Fig. 4*A*). Similarly, expression of a dominant-negative version of β-TrCP (β-TrCPΔF), which has a defective function for degradation, also prolonged the phosphorylation of HSF1 at Ser^{216} and inhibited degradation of HSF1 (Fig. 4*B, top* and *middle*). In addition, expression of β-TrCPΔF inhibited the ubiquitinylation of HSF1 (Fig. 4*B, bottom*). An immunoprecipitation assay and an *in vitro* translation assay also showed direct binding between HSF1 and β-TrCP in nocodazole-arrested mitosis (Fig. 4*C*), suggesting that the interaction of HSF1 with β-TrCP induced the degradation of phosphorylated HSF1. We further assessed whether β-TrCP binding to HSF1 requires the DSGXX(X)S phosphorylation site. Increased binding activity of HSF1S216E with β-TrCP relative to the wild-type or to the S216N mutant was observed in β-TrCP overexpressed cells. Moreover, results from a 48-hour release from thymidine double block indicated that binding of HSF1 with β-TrCP increased the degradation of HSF1, whereas the unbound form of HSF1WT, HSF1S216N, showed increased stability (Fig. 4*D*), suggesting that phosphorylated HSF1 at Ser^{216} recruited β-TrCP and degraded HSF1 itself.

HSF1 binding with Cdc20 prevents the recruitment of $SCF^{\beta\text{-TrCP}}$ and HSF1 degradation. We have previously shown that HSF1 interacted directly with Cdc20 and this interaction inhibited APC activity (17). The interaction between Cdc20 and

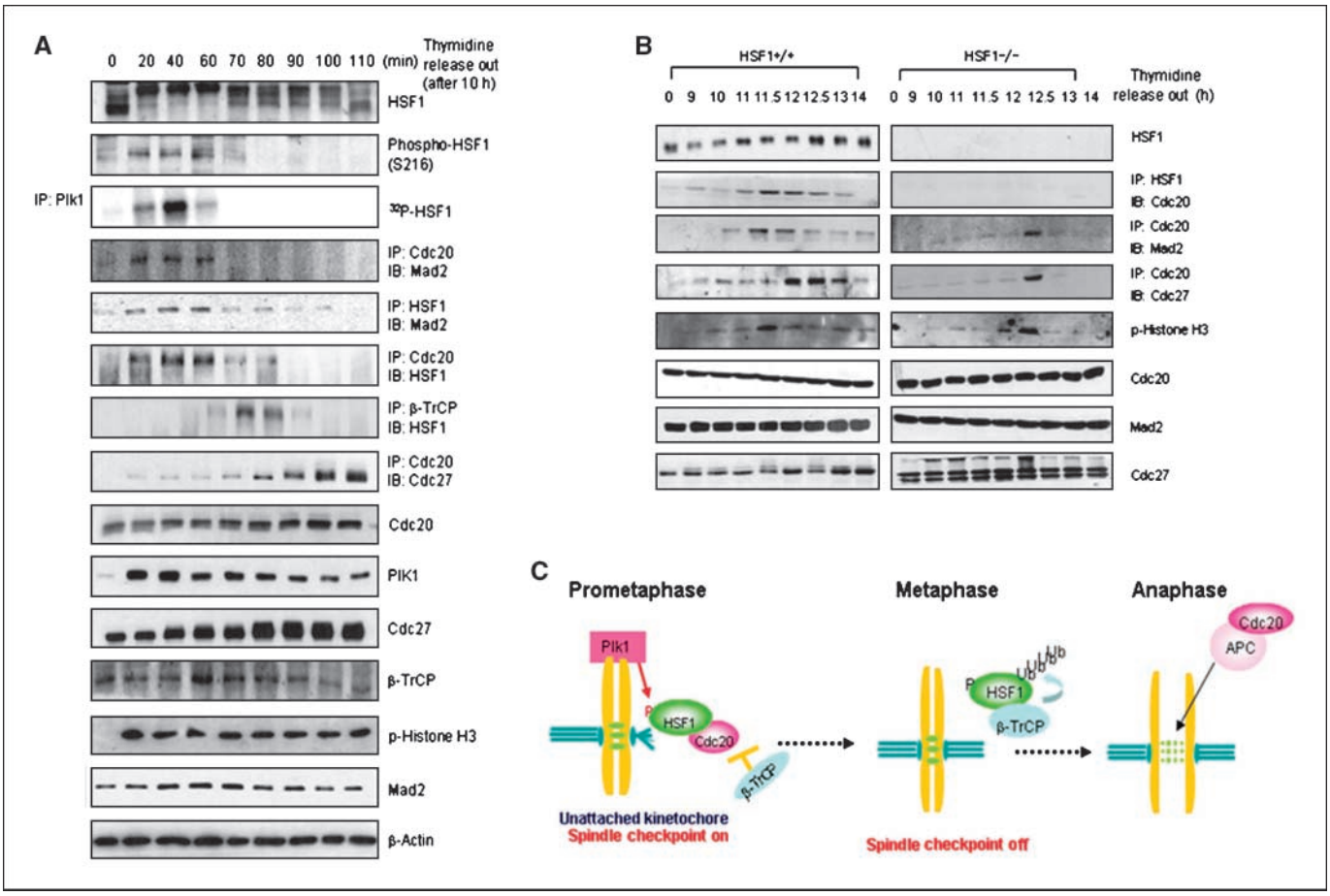

Figure 6. The phosphorylation and degradation of HSF1 is cell cycle–regulated. *A,* HOS cells were harvested at the indicated times following a double thymidine block and were released from the block. Cell lysates were subjected to immunoprecipitation and immunoblotting. *B,* HSF1+/+ and HSF1−/− MEF were harvested at the indicated times following release from the double thymidine block, and lysates were generated for immunoprecipitation and immunoblotting. *C,* a model illustrating the role of HSF1 in mitosis. During prometaphase, HSF1 is phosphorylated by Plk1 on unattached chromosomes. Phosphorylation of HSF1 can induce the spindle checkpoint activation by binding to Cdc20. In response to the bipolar attachment, phosphorylated HSF1 undergoes ubiquitin degradation through the $SCF^{\beta\text{-TrCP}}$ pathway. Ubiquitinylation of phosphorylated HSF1 facilitates the release of Cdc20, allowing it to interact with APC in anaphase.

Downloaded from http://aacrjournals.org/cancerres/article-pdf/68/18/7550/2596139/7550.pdf by guest on 13 April 2024

HSF1 disappeared upon treatment with λ-phosphatase to cell lysates (Fig. 5*A*), suggesting that phosphorylated HSF1 interacted with Cdc20. As expected, overexpression of Cdc20 inhibited the degradation of phosphorylated HSF1 after nocodazole block and release, and sustained expression of phosphorylated HSF1 at Ser^{216} was also observed (Fig. 5*B, top*). However, when HOS cells were treated with Cdc20 siRNA, degradation of HSF1 occurred (Fig. 5*B, middle*). In addition, we transfected HOS cells with Cdc20 and then synchronized the cells by use of a thymidine double block. After the block, the cells were released into fresh medium containing cycloheximide to inhibit new protein synthesis. Phosphorylated HSF1 at Ser^{216} was stabilized in Cdc20 overexpressed cells (Fig. 5*B, bottom*). To directly examine the effect of the interaction of Cdc20 on HSF1 degradation, we expressed GST-tagged Cdc20 and Cdc20ΔF (containing a deletion mutant of the HSF1 binding site) in cells expressing hemagglutinin-tagged HSF1 and Flag-tagged Plk1. Overexpression of Cdc20, but not overexpression of Cdc20ΔF, inhibited the Plk1-stimulated degradation of HSF1 (Fig. 5*C, top left*). An *in vitro* translational assay also revealed that incubation of GST-Cdc20 protein with HSF1 caused stabilization of HSF1, but incubation with GST-Cdc20ΔF protein did not stabilize HSF1 (Fig. 5*C, top right*). We also expressed GST-Cdc20 and GST-Cdc20ΔF in cells expressing hemagglutinin-tagged HSF1 to examine the relationship between the binding of HSF1 with Cdc20 and β-TrCP. Overexpression of Cdc20 inhibited HSF1-β-TrCP binding, but overexpression of Cdc20ΔF did not inhibit the binding (Fig. 5*C, bottom*), suggesting that Cdc20 blocked the binding between HSF1 and β-TrCP by binding to HSF1 itself. Taken together, these results strongly imply that Cdc20 directly binds to phosphorylated HSF1 and inhibits the Plk1-stimulated destruction of HSF1 by inhibiting the recruitment of β-TrCP.

Persistent phosphorylation of HSF1 induces mitotic arrest. To elucidate the biological significance of HSF1 phosphorylation and mitotic progression, we used heat shock on human lung carcinoma cells that showed different expression levels of HSF1. NCI-H358 showed high HSF1 expression and persistent phosphorylation of HSF1 during recovery at 37°C after heat treatment for 150 minutes at 43°C, when compared with the use of NCI-H1299 cells. Mitotic arrest by heat shock was well correlated with the phosphorylation status of HSF1, especially at Ser^{216}. Moreover, during phosphorylation of HSF1 in mitosis, induction of HSP27 and the inducible HSP70 were inhibited, indicating that the transcriptional activity of HSF1 was involved in an independent pathway for mitosis regulation by HSF1 (Supplementary Figs S5A and S5B). As compared with NCI-H1299 cells, NCI-H358 cells—after 48 hours of recovery from heat-shock—showed improper division and aneuploidy (data not shown). Moreover, NCI-H358 cells were more frequently found in the G_2-M phase after recovery from heat shock compared with NCI-H1299 cells (Supplementary Fig. S5D). Treatment of NCI-H358 cells with HSF1 siRNA inhibited mitotic arrest after heat stress (Supplementary Figs S5C and S5D), suggesting that persistent phosphorylation of HSF1 induces mitotic arrest, followed by genomic instability in lung carcinoma cells with high expression of HSF1.

Cell cycle–dependent phosphorylation and degradation of HSF1. To elucidate the fate of HSF1 in the mitotic period, the kinetics of the phosphorylation and destruction of HSF1 were monitored (Fig. 6). The association of HSF1 with Cdc20 occurred at the time points of HSF1 phosphorylation in the mitotic phase of HOS cells. The binding of HSF1 with β-TrCP occurred after the dissociation of HSF1 with Cdc20. In contrast, the interaction of Cdc20 with Cdc27 was evident after the dissociation of HSF1 with β-TrCP at the time points of phospho-HSF1 destruction (Fig. 6*A*). Given that Mad2 is a binding partner of Cdc20 at the spindle checkpoint during mitotic progression, we examined whether HSF1 contributes to the binding of Mad2 to Cdc20. HSF1 bound to Mad2 simultaneously at the time points of binding of Cdc20 with Mad2 in mitosis (Fig. 6*A*; Supplementary Fig. S6A). Mad2 siRNA inhibited the binding of Cdc20 to Mad2 or HSF1 and inhibited HSF1 phosphorylation (Supplementary Fig. S6C). Moreover, HSF1 siRNA inhibited the binding of Cdc20 to Mad2 (Supplementary Fig. S6D), indicating that the Cdc20-Mad2-HSF1 complex may be involved in the spindle checkpoint synergistically in early mitosis. When we examined these phenomena in HSF1+/+ MEF cells, similar effects were observed. However, because MEF cells are not cancer cells, these phenomena were less evident when compared with the HOS cells (Fig. 6*B*). Taken together, these results indicate that HSF1 participates in mitosis according to the following order: Plk1-mediated phosphorylation → the binding of phosphorylated HSF1 to Cdc20 → β-TrCP–mediated degradation of HSF1 → the release of Cdc20 from the HSF1 complex → the binding of Cdc20 to Cdc27 (Fig. 6*C*).

Discussion

In this study, we have identified that HSF1 is an essential checkpoint component that resides at the kinetochore during mitosis. Phosphorylated HSF1 at Ser^{216} regulates spindle pole localization and recruits the β-TrCP ubiquitin ligase, causing HSF1 destruction and allowing mitotic progression. Moreover, binding of Cdc20 to phosphorylated HSF1 regulates the degradation of phosphorylated HSF1 by the β-TrCP ubiquitin ligase.

Using chromatin immunoprecipitation combined with a DNA microarray approach in *Saccharomyces cerevisiae* after heat shock, *Bub3* and actin were identified as target genes of HSF1 (22), suggesting a possible role of HSF1 in mitotic progression. However, no direct evidence on the mechanism of HSF1 involvement in mitotic progression has been presented until now.

HSF1−/− cells showed defective mitotic progression and failure to complete cell division. Mitotic arrest after treatment with taxol and nocodazole was not observed in HSF1−/− cells (Fig. 1), whereas a higher percentage of multinucleated cells were observed, suggesting a possible role of HSF1 as a mitotic spindle checkpoint. HSF1 is localized at the kinetochore in mitosis and phosphorylation was observed in the early mitotic period. It is well known that HSF1, a phosphorylated protein, regulates the stress inducibility of *hsp* genes. Phosphorylation of serine residues Ser^{303} and Ser^{307} by mitogen-activated protein kinases and glycogen synthase kinase 3 are likely to be involved in the repression of HSF1 transcriptional activity (23). HSF1 can be potentially phosphorylated during its activation process as well, perhaps at Ser^{230}, by calcium calmodulin protein kinase II (24). However, a transcriptionally independent function is also suggested. There is a report describing that Plk1 phosphorylates HSF1 and mediates its nuclear translocation during heat stress (25). We also screened several mitotic kinases that phosphorylate HSF1 in mitosis and found that Plk1 directly phosphorylates HSF1 protein and colocalizes with HSF1 at the spindle poles during prometaphase (Fig. 2). We then conducted studies to determine which position of HSF1 was phosphorylated by Plk1. Heat stress–mediated HSF1 phosphorylation by Plk1 has been reported to occur at Ser^{419} (25). It is well known that HSF1 is phosphorylated at several serine/threonine residues. In this study,

Downloaded from http://aacrjournals.org/cancerres/article-pdf/68/18/7550/2596139/7550.pdf by guest on 13 April 2024

we found that Ser^{216} of HSF1 lies in a consensus sequence for the Plk1 phosphorylation site (E/D-X-S/T; ref. 26). To determine which residue was phosphorylated by Plk1 in mitosis, we used antibodies against phosphopeptides that could detect several serine residues of HSF1 and it was revealed that Ser^{216} of HSF1 was phosphorylated by Plk1 during mitosis (Fig. 2). Differences in the phosphorylation sites by Plk1 between mitotic regulation and for the heat stress response might be due to different mechanisms of Plk1 in mitotic regulation and other stress responses. In our system, Plk1 phosphorylated the HSF1 S419A mutant in mitosis when *in vitro* translated HSF1 protein was used as a substrate; however, the HSF1 S216A mutant was not phosphorylated, suggesting that in mitosis, Plk1 specifically phosphorylated HSF1 at the Ser^{216} residue.

Many studies have shown that phosphorylation of a substrate by a priming kinase might serve to create docking sites for Plks, which could then target other sites. Cdk1 is well known as a representative priming kinase. Recent reports have extended the number and nature of priming kinases that can direct Plk1 to its substrate such as Mapk, ATR, and Cdk1 (27). Our results suggest that Plk1 acts as a priming kinase that phosphorylates HSF1, leading to the docking of Plk1 and subsequent Ser^{221} phosphorylation of HSF1. We also determined that Ser^{221} phosphorylation at the DSGXXS motif of HSF1 is dependent on Ser^{216} phosphorylation by Plk1 (data not shown).

Phosphorylated HSF1 seemed to be degraded (Fig. 1) and treatment with a proteasome inhibitor during mitosis prolonged the HSF1 phosphorylation (Fig. 3). Recent reports have shown that SCF ubiquitin ligases are tightly coupled to protein phosphorylation, but in this case, the phosphorylation of the protein substrate is required. The action of $SCF^{\beta\text{-}TrCP}$ on its specific protein substrates usually requires phosphorylation at a specific DSGXXS motif (28). HSF1 has a DS(216p)GXXS(p) sequence and phosphorylation at Ser^{216} of HSF1 by Plk1 was observed (Fig. 2). Therefore, we hypothesized that phosphorylated HSF1 at Ser^{216} undergoes ubiquitin ligation by the $SCF^{\beta\text{-}TrCP}$ pathway. A dominant-negative mutant of Plk1 inhibited ubiquitin ligation of HSF1 and a phospho-mimic mutant of Ser^{216} showed increased ubiquitination and a shorter half-life, when compared with the phospho-deficient mutant (Fig. 3). Sustained HSF1 phosphorylation at Ser^{216} blocked destruction of HSF1 and allowed the cells to remain in a prolonged mitotic phase. Knockdown of $SCF^{\beta\text{-}TrCP}$ or transfection of $SCF^{\beta\text{-}TrCP}$ lacking the F-box domain (β-TrCPΔF), which does not have its ubiquitination function, prolonged HSF1 phosphorylation at Ser^{216} and inhibited the degradation of HSF1 (Fig. 4). Moreover, for the destruction of phosphorylated HSF1 by $SCF^{\beta\text{-}TrCP}$, a direct interaction between the two molecules was essential. Inhibition of HSF1 destruction by a knockdown of $SCF^{\beta\text{-}TrCP}$ stabilized cyclin B1 and increased the mitotic period, suggesting that HSF1 phosphorylation and destruction are tightly involved in mitotic progression.

Previously, we showed that HSF1 directly bound to Cdc20 inhibited APC activity (17). In the present study, λ-phosphatase treatment abolished the binding activity of HSF1 and Cdc20 and Cdc20 overexpression sustained HSF1 phosphorylation, indicating that binding between phosphorylated HSF1 and Cdc20 prohibited the recruitment of $SCF^{\beta\text{-}TrCP}$; therefore, the degradation of phosphorylated HSF1 was blocked.

The time kinetics of expression or interactions between the molecules during mitotic progression have revealed that in early mitosis, HSF1 was phosphorylated at Ser^{216} by Plk1 and phosphorylated HSF1 was directly bound to Cdc20, which recruited $SCF^{\beta\text{-}TrCP}$ for the destruction of HSF1. After destruction of HSF1, the Cdc20-APC interaction and transition of metaphase to anaphase were observed. In a preliminary study (Supplementary Fig. S5), HSF1 bound to Mad2, a mitotic checkpoint molecule, suggesting that HSF1 may be involved in spindle checkpoint regulation as a complex of HSF1-Mad2-Cdc20, as the knockdown of Mad2 inhibited phosphorylation of HSF1 and the interaction of HSF1 and Cdc20, as well as mitotic arrest. However, experiments that are more detailed will be needed to confirm these findings.

There is a report which showed that overexpression of dominant-negative HSF1 inhibited aneuploidy and this phenomenon was mediated by delayed breakdown of cyclin B1 (11). Our previous data also indicates that HSF1 directly binds to Cdc20 and overexpression of HSF1 induces mitotic arrest, which results in aneuploidy production (17). However, a recent report has suggested that a selective increase of several cancers occurs by functional loss of *Hsf1* in a p53-deficient mouse model (29). Therefore, HSF1 might be involved in tumorigenesis. HSF1 is also involved in normal cell cycle regulation of early mitosis independent of its transcriptional activity. Further studies should clarify the mechanism of the interaction between HSF1 and Mad2 in the spindle checkpoint regulation for normal mitotic progression, and should show how the interaction causes a switch in the normal behavior of HSF1 as a mitotic regulator to a tumorigenic factor that affects aneuploidy production and genomic instability.

Disclosure of Potential Conflicts of Interest

No potential conflicts of interest were disclosed.

Acknowledgments

Received 1/11/2008; revised 6/17/2008; accepted 6/21/2008.

Grant support: Korean Science and Engineering Foundation and by the Korean Ministry of Education, Science and Technology, through the National Nuclear Technology Program.

The costs of publication of this article were defrayed in part by the payment of page charges. This article must therefore be hereby marked *advertisement* in accordance with 18 U.S.C. Section 1734 solely to indicate this fact.

References

1. Llamazares S, Moreira A, Tavares A, et al. Polo encodes a protein kinase homolog required for mitosis in Drosophila. Genes Dev 1991;5:2153–65.
2. Lane HA, Nigg EA. Antibody microinjection reveals an essential role for human polo-like kinase 1 (Plk1) in the functional maturation of mitotic centrosomes. J Cell Biol 1996;135:1701–13.
3. Glover DM, Hagan IM, Tavares AA. Polo-like kinases: a team that plays throughout mitosis. Genes Dev 1998;12:3777–87.
4. Wasch R, Engelbert D. Anaphase-promoting complex-dependent proteolysis of cell cycle regulators and genomic instability of cancer cells. Oncogene 2005;24:1–10.
5. Irniger S, Nasmyth K. The anaphase-promoting complex is required in G1 arrested yeast cells to inhibit B-type cyclin accumulation and to prevent uncontrolled entry into S-phase. J Cell Sci 1997;110:1523–31.
6. Pfleger CM, Lee E, Kirschner MW. Substrate recognition by the Cdc20 and Cdh1 components of the anaphase-promoting complex. Genes Dev 2001;15:2396–407.
7. Kotani S, Tanaka H, Yasuda H, Todokoro K. Regulation of APC activity by phosphorylation and regulatory factors. J Cell Biol 1999;146:791–800.
8. Rudner AD, Murray AW. Phosphorylation by Cdc28 activates the Cdc20-dependent activity of the anaphase-promoting complex. J Cell Biol 2000;149:1377–90.
9. Lahav-Baratz S, Sudakin V, Ruderman JV, Hershko A. Reversible phosphorylation controls the activity of cyclosome-associated cyclin-ubiquitin ligase. Proc Natl Acad Sci U S A 1995;92:9303–7.
10. Pirkkala L, Nykanen P, Sistonen L. Roles of the heat shock transcription factors in regulation of the

Downloaded from http://aacrjournals.org/cancerres/article-pdf/68/18/7550/2596139/7550.pdf by guest on 13 April 2024

heat shock response and beyond. FASEB J 2001;15:1118–31.
11. Wang Y, Theriault JR, He H, Gong J, Calderwood SK. Expression of a dominant negative heat shock factor-1 construct inhibits aneuploidy in prostate carcinoma cells. J Biol Chem 2004;279:32651–9.
12. Sarge KD, Murphy SP, Morimoto RI. Activation of heat shock gene transcription by heat shock factor 1 involves oligomerization, acquisition of DNA-binding activity, and nuclear localization and can occur in the absence of stress. Mol Cell Biol 1993;13:1392–407.
13. Cotto J, Fox S, Morimoto R. HSF1 granules: a novel stress-induced nuclear compartment of human cells. J Cell Sci 1997;110:2925–34.
14. Jolly C, Morimoto R, Robert-Nicoud M, Vourc'h C. HSF1 transcription factor concentrates in nuclear foci during heat shock: relationship with transcription sites. J Cell Sci 1997;110:2935–41.
15. Jolly C, Usson Y, Morimoto RI. Rapid and reversible relocalization of heat shock factor 1 within seconds to nuclear stress granules. Proc Natl Acad Sci U S A 1999;96:6769–74.
16. Jolly C, Konecny L, Grady DL, et al. *In vivo* binding of active heat shock transcription factor 1 to human chromosome 9 heterochromatin during stress. J Cell Biol 2002;156:775–81.
17. Lee YJ, Lee HJ, Bae S, et al. A novel function for HSF1-induced mitotic exit failure and genomic instability through direct interaction between HSF1 and Cdc20. Oncogene 2008;27:2999–3009.
18. Lee YJ, Lee DH, Cho CK, et al. HSP25 inhibits protein kinase Cδ-mediated cell death through direct interaction. J Biol Chem 2005;280:18108–19.
19. Song MS, Song SJ, Ayad NG, et al. The tumour suppressor RASSF1A regulates mitosis by inhibiting the APC-Cdc20 complex. Nat Cell Biol 2004;6:129–37.
20. Bagatell R, Paine-Murrieta GD, Taylor CW, et al. Induction of a heat shock factor 1-dependent stress response alters the cytotoxic activity of hsp90-binding agents. Clin Cancer Res 2000;6:3312–8.
21. Nakayama KI, Nakayama K. Regulation of the cell cycle by SCF-type ubiquitin ligases. Semin Cell Dev Biol 2005;16:323–33.
22. Hahn JS, Thiele DJ. Activation of the *Saccharomyces cerevisiae* heat shock transcription factor under glucose starvation conditions by Snf1 protein kinase. J Biol Chem 2004;279:5169–76.
23. Yang XJ, Gregoire S. A recurrent phospho-sumoyl switch in transcriptional repression and beyond. Mol Cell 2006;23:779–86.
24. Holmberg CI, Hietakangas V, Mikhailov A, et al. Phosphorylation of serine 230 promotes inducible transcriptional activity of heat shock factor 1. EMBO J 2001;20:3800–10.
25. Kim SA, Yoon JH, Lee SH, Ahn SG. Polo-like kinase 1 phosphorylates heat shock transcription factor 1 and mediates its nuclear translocation during heat stress. J Biol Chem 2005;280:12653–7.
26. Nakajima H, Toyoshima-Morimoto F, Taniguchi E, Nishida E. Identification of a consensus motif for Plk (Polo-like kinase) phosphorylation reveals Myt1 as a Plk1 substrate. J Biol Chem 2003;278:25277–80.
27. van Vugt MA, Medema RH. Getting in and out of mitosis with Polo-like kinase-1. Oncogene 2005;24:2844–59.
28. Vodermaier HC. APC/C and SCF: controlling each other and the cell cycle. Curr Biol 2004;14:R787–96.
29. Min JN, Huang L, Zimonjic DB, Moskophidis D, Mivechi NF. Selective suppression of lymphomas by functional loss of Hsf1 in a p53-deficient mouse model for spontaneous tumors. Oncogene 2007;26:5086–97.

Downloaded from http://aacrjournals.org/cancerres/article-pdf/68/18/7550/2596139/7550.pdf by guest on 13 April 2024